Improved age estimates for Holocene Ko-g and Ma-f~j tephras in northern Japan using Bayesian statistical modelling

Xuan-Yu Chen [a,b,c*], Simon P.E. Blockley [b], Richard A. Staff [d], Yi-Gang Xu [a], Martin A. Menzies [c]

[a] State Key Laboratory of Isotope Geochemistry and CAS Center for Excellence in Deep Earth Science, Guangzhou Institute of Geochemistry, Chinese Academy of Sciences, Guangzhou, 510640, China

[b] Department of Geography, Royal Holloway University of London, Egham, Surrey, TW20 0EX, UK

[c] Department of Earth Sciences, Royal Holloway University of London, Egham, Surrey, TW20 0EX, UK

[d] Scottish Universities Environmental Research Centre (SUERC), University of Glasgow, East Kilbride, G75 0QF, UK

Abstract

The Ko-g and Ma-f~j tephras are two key isochronous marker layers in northern Japan, which are from the largest Plinian eruptions of Komagatake volcano (VEI=5) and Mashu caldera (VEI=6), respectively. Despite extensive radiocarbon studies associated with the two tephras, individual calibrated results show considerable variations and thus accurate ages of these important eruptions remain controversial. Bayesian statistical approaches to calibrating radiocarbon determinations have proven successful in increasing accuracy and sometimes precision for dating tephras, which is achieved through the incorporation of additional stratigraphic information and the combination of evidence from multiple records. Here we use Bayesian approaches to analyse the proximal and distal information associated with the two tephra markers. Through establishing phase and deposition models, we have taken into account all of the currently available stratigraphic and chronological information. The cross-referencing of phase models with the deposition model allows the refinement of eruption ages and the deposition model itself. Using this we are able to provide the most robust current age estimates for the two tephra layers. The Ko-g and Ma-f~j tephras are hereby dated to 6657-6505 (95.4%; 6586±40, μ±σ) cal yr BP, and 7670-7395 (95.4%; 7532±72, μ±σ) cal yr BP, respectively. These updated age determinations underpin the reported East Asian Holocene tephrostratigraphic framework, and allow sites where the tephra layers are present to be dated more precisely and accurately. Our results encourage further applications of Bayesian modelling techniques in the volcanically active East Asian region.

1 Introduction

A robust chronological framework is essential for the investigation of past environmental and climatic changes recorded in various sedimentary archives (Brauer et al., 2014). To this end, the past decades have witnessed considerable progress regarding the use of tephra isochrons as a dating and correlation tool for precise palaeoclimatic and environmental reconstruction (e.g., Davies et al., 2010; Lane et al., 2013; Berben et al., 2020). The major advantages of tephra isochrons are their ability to perfectly synchronise records, and that the most robust age estimate for a tephra can be transferred to other records where the tephra is identified (Lowe, 2011). This generates the motivation to produce ever more precise and accurate age estimates for key tephra markers.

The mid-Holocene Ko-g and Ma-f~j tephras are two major isochronous markers in northern Japan (Furukawa and Nanayama, 2006; Nakamura, 2016; Razzhigaeva et al., 2016), which form an important part of the integrated East Asian tephrostratigraphic framework (Chen et al., 2020). These tephras have been dated extensively using the radiocarbon (^{14}C) method (e.g., Okuno et al., 1999; Nakamura and Hirakawa, 2004; Yoshimoto et al., 2008; Yamamoto et al., 2010; Razzhigaeva et al., 2016), yet the results yield considerable variations, diminishing the chronological significance of the tephras. This is due to the fact that ^{14}C calibrated dates derived from individual samples are more likely to suffer from contamination and calibration issues (Lowe and Walker, 2000). In contrast, Bayesian modelling approaches to calibrating radiocarbon determinations have been developed to allow the incorporation of prior information (e.g., stratigraphic ordering) and the combination of evidence from multiple records (Buck et al., 1991, 1992; Bronk Ramsey, 1994, 1995, 2008, 2009a). These approaches have proven very successful in generating robust chronologies for tephra layers and a range of other sedimentary records, and thus have been widely used in many regions (e.g., Buck et al., 2003; Blockley et al., 2004, 2007, 2008a, 2008b; Wohlfarth et al., 2006; Petrie and Torrence, 2008; Schiff et al., 2008; Smith et al., 2011, 2013; Lowe et al., 2013; Vandergoes et al., 2013; Macken et al., 2013; Xu et al., 2013; Bronk Ramsey et al., 2015; Egan et al., 2015; Chen et al., 2016; McLean et al., 2016, 2018, 2020a, 2020b; Albert et al., 2018, 2019; Sun et al., 2018, 2019).

Here we use Bayesian modelling approaches to analyse ^{14}C dates reported for the Ko-g and Ma-f~j tephras. Given that previous age estimates for these eruptions were all based on individual calibrated determinations, the aim of this article is to combine the chronological information through a statistically robust approach, in order to provide coherent calendar ages for the tephras. Our results demonstrate that tephra age estimates can be refined when properly modelled using all available information, and that these tephras provide critical elements of a broader regional Holocene tephrostratigraphic framework.

2 Background

2.1 Ko-g tephra

The Ko-g tephra originated from the Komagatake volcano in SW Hokkaido (Fig. 1), and was the product of its largest Holocene eruption (VEI=5, Nakamura and Hirakawa, 2004; Yoshimoto et al., 2008). Having a bulk volume of 2.4-3.8 km^3 (Nakamura and Hirakawa, 2004), the eruption dispersed tephra towards the ENE (Furukawa and Nanayama, 2006). In the southern Kuril Islands (ca. 450 km ENE of the source), the tephra has been identified as a visible layer in a peat sequence (Razzhigaeva et al., 2016), whereas in Rebun Island (ca. 370 km N of the source) the tephra occurs as a non-visible ash layer identified in lake sediments (Chen et al., 2019). Based on reviewing its occurrences, Chen et al. (2020) suggested that the tephra plausibly covered the entirety of Hokkaido Island (Fig. 1).

A range of studies have attempted to date the tephra using the ^{14}C method, and the individual calibrated results yielded various but overlapping age ranges. For example, Nakamura and Hirakawa (2004) dated plant material and wood immediately above and below the Ko-g unit, with one of the samples yielding the most precise age of 6661-6451 cal yr BP (95.4%), while the other two dates exhibited larger uncertainty. In contrast, Razzhigaeva et al. (2016) provided an older date that had a comparable error range (6844-6635 cal yr BP; 95.4%). Moreover, Yoshimoto et al. (2008) reported a date derived from charcoal within the bottom part of the tephra unit overlapping the two dates mentioned above, but with significantly larger uncertainty (7158-6552 cal yr BP; 95.4%). Table 1 summarises the detailed stratigraphic and chronological information of the published ^{14}C dates associated with the Ko-g tephra. All the raw dates are re-calibrated in this study using the latest IntCal20 calibration curve (Reimer et al., 2020), in order to allow direct comparison of the resultant calendar ages.

2.2 Ma-f~j tephra

The Ma-f~j tephra originated from Mashu caldera in eastern Hokkaido (Fig. 1), and was the product of its caldera forming eruption (VEI=6, Crosweller et al., 2012; Katsui, 1963). The eruption consisted of five eruptive phases, ejecting a total bulk tephra volume of 18.6 km^3 (Kishimoto et al., 2009). Initially, the volcano erupted pulverulent solidified lavas forming an ash-fall unit, Ma-j. This was followed by successive pumice-fall units Ma-i and Ma-h&g with white and light grey colours, respectively. The activity ended with a pyroclastic flow containing large amounts of grey pumice and ash with lithic fragments (Ma-f) (Katsui, 1963; Katsui et al., 1975). The Ma-f~j tephra was dispersed towards the ESE, with the pumice-fall units (Ma-i and Ma-g) being found as 10 cm thick layers ca. 100 km to the east of the source (Katsui, 1963). Recently, Razzhigaeva et al. (2016) identified the visible Ma-f~j tephra in eleven peat sequences in the southern Kuril Islands, ca. 200 km to the east of the volcano. In addition, Chen et al. (2019) reported the presence of Ma-f~j cryptotephra in Lake Kushu, Rebun Island ca. 350 km NW of the volcano (Fig. 1). These new discoveries extend the known dispersal of the tephra, indicating that it has significant potential to be developed as a regional stratigraphic marker (Chen et al., 2020).

Radiocarbon dating of charcoals preserved within the tephra and humus from underlying soils have provided various dates for the eruption, ranging from 6460 to

8870 ^{14}C yr BP (Table 1). For instance, charcoals within the uppermost Ma-f unit yielded ages of 7681-7483 and 7566-7277 cal yr BP (95.4%; Yamamoto et al., 2010), whereas samples from soils immediately below the tephra provided dates of 7920-7666 cal yr BP (95.4%; Yamamoto et al., 2010), 8180-7978 cal yr BP (95.4%; Razzhigaeva et al., 2016) and 8598-8380 cal yr BP (95.4%; Nakamura and Hirakawa, 2004) that are significantly older (Table 1).

2.3 Lake Kushu in Rebun Island

Rebun Island is situated in the northeastern part of the Sea of Japan, ca. 45 km west of the northern coast of Hokkaido (Fig. 1). Lake Kushu (45°25′55″N, 141°02′13″E, 4 m.a.s.l.) is a coastal freshwater lake located in the northern part of the island about 300 m from the coast (Fig. 1). The lake is surrounded by dense vegetation, which effectively limits any sediment in-washing. Dominant sources of sediment include autochthonous biological productivity, aeolian input and minor fluvial input (Schmidt et al., 2016).

The RK12 sediment core was extracted from Lake Kushu in February 2012. Two parallel cores, RK12-01 and RK12-02, were recovered using a hydro-pressure thin-walled piston corer. The composite RK12 sequence spans ca. 19.5 m and is composed of continuous, partly laminated, organic-rich sediments. A total of fifty-seven bulk sediment 1 cm samples throughout the composite sequence were processed for AMS radiocarbon dating, and the results allowed the construction of the RK12 age model (Müller et al., 2016). Detailed cryptotephra analysis was performed on the Holocene sediments, which revealed key tephra markers from multiple regions, including the Hokkaido Ko-g and Ma-f~j tephras (Chen et al., 2016, 2019).

3 Bayesian modelling of tephra ages

As previously outlined, attempts have been made to date the Ko-g and Ma-f~j tephras using ^{14}C dating, however, individual calibrated determinations show considerable variations between studies (see Table 1). Bayesian approaches to data analysis provide a means to increase the reliability of chronological results through the inclusion of additional stratigraphic information and the combination of evidence from multiple records. To this end, we follow the method outlined by Blockley et al. (2008b) and have applied Bayesian approaches to integrate chronological and stratigraphic data from both proximal and distal sources, attempting to provide the most robust age estimates for the two tephra layers. All the modelling exercises described in the following sections have been carried out using OxCal v4.4.4 (Bronk Ramsey, 2021), applying the latest consensus calibration curve, IntCal20 (Reimer et al., 2020).

3.1 Phase modelling

Chronological information for the Ko-g tephra from proximal sites is summarised in Table 1. We constructed a two *Phase* Bayesian model (Buck et al., 1992) for the Ko-g tephra using the reported ages and the stratigraphic relationships between the dated materials and the tephra layer. These two model phases comprise: (1) a phase of dates derived from materials sampled within or immediately below the tephra layer, and (2) a phase of dates for materials known to stratigraphically overlay the tephra layer. The logic of the model is that although the Ko-g eruption is considered as a single event in geological terms, the sampling resolution of the dated materials allows them to be grouped into different phases. We consider the dates in phase one to be slightly older than that of the eruption, and the phase is therefore named the ‘pre-eruption’ phase. In contrast, phase two contains dates younger than that of the eruption and is named the 'post eruption' phase. The dates within each phase are stratigraphically unordered in relation to each other, given that they are from different records and their relative stratigraphic order is unknown. A "General" *Outlier_Model* is applied to statistically determine any outliers and down-weight any such ages so that they do not exert undue influence on the refined calculated age (Bronk Ramsey, 2009b). The *Tau_Boundary* function is applied to constrain the beginning and the end of the sequence, taking account of the fact that the ^{14}C samples are more likely to closely pre- or post-date the eruption, with a decreasing probability that the ages are more markedly older or younger than the eruption age, respectively (e.g., Egan et al., 2015; Davies et al., 2016). The pre- and post- eruption phases are separated by a *Boundary*, whose date indicates the timing of the eruption. The output for this model is presented in Fig. 2a, along with the posterior outlier probabilities [O] for each sample. In this model, there are no significant outliers detected. The 95.4% confidence interval for the modelled age of the Ko-g tephra, integrating available chronological and stratigraphic data from multiple proximal records, is 6651-6446 cal yr BP.

The Ma-f~j tephra, dated by materials within and below the deposit, has scattered age determinations ranging from ca. 6.5 to 8.9 ^{14}C ka BP (Table 1). The lack of any overlying dates for the tephra could have an impact on the modelled eruption age. This could lead to, for example, a longer tail trending towards the younger ages, simply because the model is not constrained from above. Nevertheless, it is still worth utilising the Bayesian approach to integrate available ^{14}C dates for the tephra. Here we again take the stratigraphically unordered but related group of dates as a *Phase*. The *Sequence* model for the Ma-f~j tephra has only one phase, as we consider that ages of samples from within the tephra also (closely) pre-date the eruption. This is because although the plants were killed by the pyroclastic deposits generated during the eruption, they are nevertheless more likely to have recorded the atmospheric $^{14}CO_2$ level before the eruption happened, and potentially for many decades depending on species. As such they are grouped with dates from below the tephra, in a 'pre-eruption' phase. We apply a "General" *Outlier_Model* (Bronk Ramsey, 2009b) to the *Sequence* model and the prior outlier probability for each ^{14}C date is set to be 5%. A *Tau_Boundary* is placed at the beginning of the sequence, as with that in the Ko-g model. The output for this Ma-f~j model is presented in Fig. 2b, with no significant outliers detected. A date with a posterior outlier probability of 7% is automatically down-weighted by the *Outlier_Model* in proportion to its likelihood of being outlying. The boundary at the end of the sequence indicates the modelled eruption age. The 95.4% confidence interval for the modelled age of the Ma-f~j tephra, 7550-7128 cal yr BP, is now constrained by the stratigraphic relationships between the dated samples and the tephra itself.

3.2 Deposition modelling

In order to further resolve the timing of the two tephras, we used evidence from a long depositional sequence where it is possible to incorporate more information. The identification of the Ko-g and Ma-f~j cryptotephra layers in the ^{14}C dated Lake Kushu record (Chen et al., 2019) means that it is possible to incorporate the modelled phases within a formal deposition model (Bronk Ramsey, 2008), as opposed to just using the stratigraphic ordering information from the phase modelling, above. To achieve this, we constructed a formal Bayesian age model based on the fifty-seven AMS ^{14}C dates from the Kushu sequence (Müller et al., 2016). The model utilises a *P_Sequence* deposition model, which is appropriate for lake sediments and assumes that deposition is a Poison process (Bronk Ramsey, 2008). With a variable *k* parameter (Bronk Ramsey and Lee, 2013), the analysis is able to find the most appropriate *k* value (rigidity) of the

P_Sequence automatically. A precise age for the B-Tm tephra (946 CE; Oppenheimer et al., 2017) is imposed in the uppermost section of the model, given its identification in the RK12 record (Chen et al., 2016). The apparent age reversals that were regarded as outliers (see Müller et al., 2016) are removed from the model. A "General" *Outlier_Model* (Bronk Ramsey, 2009b) is applied to detect and down-weight any further outliers. Most importantly, we have the two *Phase* models of the Ko-g and Ma-f~j cross-referenced into the *P_Sequence* at the positions where the tephras were identified (see supplementary material for model coding). This allows us to make use of all currently available chronological and stratigraphic information from both proximal and distal sources to provide the optimal chronology for these important eruptions. The 95.4% Highest Probability Density (HPD) ranges for the deposition model and the tephra layers are illustrated in Fig. 3. The final modelled dates for the Ko-g and Ma-f~j tephras are 6657-6505 cal yr BP and 7670-7395 cal yr BP (95.4%), respectively. For comparison, we also establish a deposition model based purely on the Kushu ^{14}C dates without cross-referencing the two phase models, which however shows much less precise eruption ages for the two tephras (Table 2).

4 Discussion

Utilising the proximal stratigraphic information (i.e. ordering of events) alone, the phase modelling exercise provides an age of 6651-6446 cal yr BP (95.4%; or 6545±52, $\mu\pm\sigma$) for the Ko-g tephra. This age estimate has been subsequently refined to 6657-6505 cal yr BP (95.4%; or 6586±40, $\mu\pm\sigma$) when additional constraints from the Kushu sequence have been implemented (Fig. 3). This final modelled date is in good accordance with most of the reported ages for the tephra, but also indicates that an older age (GIN-8945; Razzhigaeva et al., 2016) should no longer be referred to as eruption age, given the 1 cm offset between the dated material and the tephra itself (Fig. 4a). In addition, cross-referencing the Ko-g phase model has helped improve the Kushu deposition model, as the comparative deposition model based purely on Kushu ^{14}C dates has produced a much less precise date for the Ko-g eruption (Table 2). Most importantly, our final modelled result incorporates all of the currently available information and has the highest precision (152 years' uncertainty, 95.4% confidence interval) compared to the previous results that possess greater uncertainties ranging from ca. 210 years to over 600 years (Fig. 4a).

In a similar manner, the Ma-f~j tephra has a phase modelled result of 7550-7128 cal yr BP (95.4%; or 7348±111, μ±σ). This age estimate possesses relatively large uncertainty range, which is due to the lack of an upper limit defined for the eruption boundary (Fig. 2b). The incorporation of the phase model into the Kushu deposition model has added an upper boundary for the eruption age (Fig. 3), which constrains the modelled age from trending towards an unrealistically young minimum. In this case, information from both the phase and deposition models together informs the eruption age, and the age is refined to 7670-7395 cal yr BP (95.4%; or 7532±72, μ±σ). Our modelled result suggests that one of the most precise published dates (8180-7978 cal yr BP, GIN-13454; Razzhigaeva et al., 2016), along with other age estimates that are older than ca. 7.7 cal ka BP, should no longer be referred to as eruption ages for the Ma-f~j, though they were derived from samples within or immediately below the tephra (Fig. 4b). One critical issue here may be the choice of dated materials which were, however, not specified in the original publication (Table 1). Although our modelled date is less precise than some of the published dates (Fig. 4b), it represents the current most accurate age estimate for the Ma-f~j tephra.

The modelling exercises conducted in this study demonstrate the potential of Bayesian analysis for testing and improving eruption ages for tephras in northern Japan. Integrating stratigraphic and chronological information from multiple sources using Bayesian approaches has made it possible to refine tephra age estimates. Our results underpin the on-going construction of a regional tephrostratigraphic framework, and would facilitate the use of these tephra isochrons as a key chronological tool for precise palaeoenvironmental reconstruction and other Quaternary studies in the region. Therefore, these Bayesian approaches are recommended to be more widely applied in Japan and the wider East Asian region

5 Conclusion

Bayesian modelling approaches have proven very successful in generating robust chronologies for tephra isochrons. These techniques are able to directly integrate chronological and stratigraphic information from multiple sources. In this study, we apply the Bayesian approaches to two major Holocene tephra markers in northern Japan, the Ko-g and Ma-f~j tephras. The integration of phase models based on proximal data into the deposition model of a distal archive allows the refinement of eruption ages and the deposition model itself. Using this we date the Ko-g tephra to 6657-6505 (95.4%; 6586±40, $\mu\pm\sigma$) cal yr BP, which is currently the most precise and accurate age estimate for the tephra marker. In addition, the Ma-f~j tephra is dated to 7670-7395 (95.4%; 7532±72, $\mu\pm\sigma$) cal yr BP, which represents the most accurate current age estimate and helps rule out several published eruption ages that are apparently too old. These new age determinations update the East Asian Holocene tephrostratigraphic framework reported in Chen et al. (2020), and allow sites where the tephra layers are present to be dated more robustly. We advocate that the Bayesian approaches should be more widely applied in the volcanically active East Asian region.

Acknowledgements

This study was supported by Chinese Academy of Sciences Strategic Priority Research Program (B) (XDB18000000) and the External Cooperation Program of the Bureau of International Co-operation, CAS (Grant No. 132744KYSB20130005). XYC would like to acknowledge the RHUL-China Scholarship awarded to him by RHUL under the collaboration scheme between GIGCAS and RHUL. We would like to thank two anonymous reviewers for their constructive feedback on an earlier version of the manuscript, and Prof. Siwan Davies for handling the manuscript. This is contribution No. IS-3054 from GIGCAS.

References

Albert, P.G., Smith, V.C., Suzuki, T., McLean, D., Tomlinson, E.L., Miyabuchi, Y., Kitaba, I., Mark, D.F., Moriwaki, H. and Nakagawa, T., 2019. Geochemical characterisation of the Late Quaternary widespread Japanese tephrostratigraphic markers and correlations to the Lake Suigetsu sedimentary archive (SG06 core). Quat Geochronol.

Albert, P.G., Smith, V.C., Suzuki, T., Tomlinson, E.L., Nakagawa, T., McLean, D., Yamada, M., Staff, R.A., Schlolaut, G. and Takemura, K., 2018. Constraints on the frequency and dispersal of explosive eruptions at Sambe and Daisen volcanoes (South-West Japan Arc) from the distal Lake Suigetsu record (SG06 core). Earth-Sci Rev, 185: 1004-1028.

Berben, S.M.P., Dokken, T.M., Abbott, P.M., Cook, E., Sadatzki, H., Simon, M.H. and Jansen, E., 2020. Independent tephrochronological evidence for rapid and synchronous oceanic and atmospheric temperature rises over the Greenland stadial-interstadial transitions between ca. 32 and 40 ka b2k. Quaternary Science Reviews, 236: 106277.

Blockley, S.P.E., Blaauw, M., Bronk Ramsey, C. and van der Plicht, J., 2007. Building and testing age models for radiocarbon dates in Lateglacial and Early Holocene sediments. Quaternary Science Reviews, 26(15): 1915-1926.

Blockley, S.P.E., Bronk Ramsey, C., Lane, C.S. and Lotter, A.F., 2008a. Improved age modelling approaches as exemplified by the revised chronology for the Central European varved lake Soppensee. Quaternary Science Reviews, 27(1): 61-71.

Blockley, S.P.E., Bronk Ramsey, C. and Pyle, D.M., 2008b. Improved age modelling and high-precision age estimates of late Quaternary tephras, for accurate palaeoclimate reconstruction. Journal of Volcanology and Geothermal Research, 177(1): 251-262.

Blockley, S.P.E., Lowe, J.J., Walker, M.J.C., Asioli, A., Trincardi, F., Coope, G.R. and Donahue, R.E., 2004. Bayesian analysis of radiocarbon chronologies: examples from the European Late-glacial. Journal of Quaternary Science, 19(2): 159-175.

Brauer, A., Hajdas, I., Blockley, S.P.E., Bronk Ramsey, C., Christl, M., Ivy-Ochs, S., Moseley, G.E., Nowaczyk, N.N., Rasmussen, S.O., Roberts, H.M., Spötl, C., Staff, R.A. and Svensson, A., 2014. The importance of independent chronology in integrating records of past climate change for the 60–8 ka INTIMATE time interval. Quaternary Science Reviews, 106: 47-66.

Bronk Ramsey, C., 1994. Analysis of Chronological Information and Radiocarbon Calibration : The Program OxCal. Archaeological Computing Newsletter, 41: 11-16.

Bronk Ramsey, C., 1995. Radiocarbon calibration and analysis of stratigraphy: The OxCal program. Radiocarbon, 37(2): 425-430.

Bronk Ramsey, C., 2008. Deposition models for chronological records. Quaternary Science Reviews, 27(1–2): 42-60.

Bronk Ramsey, C., 2009a. Bayesian analysis of radiocarbon dates. Radiocarbon, 51(1): 337-360.

Bronk Ramsey, C., 2009b. Dealing with outliers and offsets in radiocarbon dating. Radiocarbon, 51(3): 1023-1045.

Bronk Ramsey, C., 2021. OxCal 4.4.4. Available from: http://c14.arch.ox.ac.uk/oxcal.

Bronk Ramsey, C., Albert, P.G., Blockley, S.P.E., Hardiman, M., Housley, R.A., Lane, C.S., Lee, S., Matthews, I.P., Smith, V.C. and Lowe, J.J., 2015. Improved age estimates for key Late Quaternary European tephra horizons in the RESET lattice. Quaternary Science Reviews, 118: 18-32.

Bronk Ramsey, C. and Lee, S., 2013. Recent and planned developments of the program OxCal. Radiocarbon, 55(2): 720-730.

Buck, C.E., Higham, T.F.G. and Lowe, D.J., 2003. Bayesian tools for tephrochronology. The Holocene, 13(5): 639-647.

Buck, C.E., Kenworthy, J.B., Litton, C.D. and Smith, A.F.M., 1991. Combining archaeological and radiocarbon information: a Bayesian approach to calibration. Antiquity, 65(249): 808-821.

Buck, C.E., Litton, C.D. and Smith, A.F.M., 1992. Calibration of radiocarbon results pertaining to related archaeological events. Journal of Archaeological Science, 19(5): 497-512.

Chen, X.-Y., Blockley, S.P.E., Tarasov, P.E., Xu, Y.-G., McLean, D., Tomlinson, E.L., Albert, P.G., Liu, J.-Q., Müller, S., Wagner, M. and Menzies, M.A., 2016. Clarifying the distal to proximal tephrochronology of the Millennium (B–Tm) eruption, Changbaishan Volcano, northeast China. Quat Geochronol, 33: 61-75.

Chen, X.-Y., Blockley, S.P.E., Xu, Y.-G. and Menzies, M.A., 2020. Holocene tephrostratigraphic framework and monsoon evolution of East Asia: Key tephra beds for synchronising palaeoclimate records. Quaternary Science Reviews, 242: 106467.

Chen, X.-Y., McLean, D., Blockley, S.P.E., Tarasov, P.E., Xu, Y.-G. and Menzies, M.A., 2019. Developing a Holocene tephrostratigraphy for northern Japan using the sedimentary record from Lake Kushu, Rebun Island. Quaternary Science Reviews, 215: 272-292.

Crosweller, H.S., Arora, B., Brown, S.K., Cottrell, E., Deligne, N.I., Guerrero, N.O., Hobbs, L., Kiyosugi, K., Loughlin, S.C., Lowndes, J., Nayembil, M., Siebert, L., Sparks, R.S.J., Takarada, S. and Venzke, E., 2012. Global database on large magnitude explosive volcanic eruptions (LaMEVE). Journal of Applied Volcanology, 1(1): 4.

Davies, L.J., Jensen, B.J.L., Froese, D.G. and Wallace, K.L., 2016. Late Pleistocene and Holocene tephrostratigraphy of interior Alaska and Yukon: Key beds and chronologies over the past 30,000 years. Quaternary Science Reviews, 146: 28-53.

Davies, S.M., Wastegård, S., Abbott, P., Barbante, C., Bigler, M., Johnsen, S.J., Rasmussen, T.L., Steffensen, J.P. and Svensson, A., 2010. Tracing volcanic events in the NGRIP ice-core and synchronising North Atlantic marine records during the last glacial period. Earth and Planetary Science Letters, 294(1-2): 69-79.

Egan, J., Staff, R. and Blackford, J., 2015. A high-precision age estimate of the Holocene Plinian eruption of Mount Mazama, Oregon, USA. The Holocene, 25(7): 1054-1067.

Furukawa, R. and Nanayama, F., 2006. Holocene pyroclastic fall deposits along the Pacific coastal region of eastern Hokkaido. Bulletin of Volcanological Society of Japan, 51(6): 351-371 (in Japanese with English abstract).

Katsui, Y., 1963. Evolution and magmatic history of some Krakatoan calderas in Hokkaido, Japan. Journal of the Faculty of Science, Hokkaido University. Series 4, Geology and mineralogy, 11(4): 631-650.

Katsui, Y., Ando, S. and Inaba, K., 1975. Formation and magmatic evolution of Mashu volcano, east Hokkaido, Japan. Journal of the Faculty of Science, Hokkaido University. Series 4, Geology and mineralogy, 16(4): 533-552.

Kishimoto, H., Hasegawa, T., Nakagawa, M. and Wada, K., 2009. Tephrostratigraphy and eruption style of Mashu volcano, during the last 14,000 years, eastern Hokkaido, Japan. Bulletin of the Volcanological Society of Japan, 54: 15-36 (in Japanese with English abstract).

Lane, C.S., Brauer, A., Blockley, S.P.E. and Dulski, P., 2013. Volcanic ash reveals time-transgressive abrupt climate change during the Younger Dryas. Geology, 41(12): 1251-1254.

Lowe, D.J., 2011. Tephrochronology and its application: A review. Quat Geochronol, 6(2): 107-153.

Lowe, D.J., Blaauw, M., Hogg, A.G. and Newnham, R.M., 2013. Ages of 24 widespread tephras erupted since 30,000 years ago in New Zealand, with re-evaluation of the timing and palaeoclimatic implications of the Lateglacial cool episode recorded at Kaipo bog. Quaternary Science Reviews, 74: 170–194.

Lowe, J.J. and Walker, M.J., 2000. Radiocarbon dating of the last glacial-interglacial transition (Ca. 14-9 ^{14}C ka BP) in terrestrial and marine records; the need for new quality assurance protocols. Radiocarbon, 42: 53-68.

Machida, H. and Arai, F., 2003. Atlas of Tephra in and around Japan, Revised ed. University of Tokyo press, Tokyo, Japan (In Japanese).

Macken, A.C., Staff, R.A. and Reed, E.H., 2013. Bayesian age-depth modelling of Late Quaternary deposits from Wet and Blanche Caves, Naracoorte, South Australia: A framework for comparative faunal analyses. Quat Geochronol, 17: 26-43.

McLean, D., Albert, P.G., Nakagawa, T., Staff, R.A., Suzuki, T. and Smith, V.C., 2016. Identification of the Changbaishan 'Millennium'(B-Tm) eruption deposit in the Lake Suigetsu (SG06) sedimentary archive, Japan: synchronisation of hemispheric-wide palaeoclimate archives. Quaternary Science Reviews, 150: 301-307.

McLean, D., Albert, P.G., Nakagawa, T., Suzuki, T., Staff, R.A., Yamada, K., Kitaba, I., Haraguchi, T., Kitagawa, J. and Smith, V.C., 2018. Integrating the Holocene tephrostratigraphy for East Asia using a high-resolution cryptotephra study from Lake Suigetsu (SG14 core), central Japan. Quaternary Science Reviews, 183: 36-58.

McLean, D., Albert, P.G., Suzuki, T., Nakagawa, T., Kimura, J.-I., Chang, Q., MacLeod, A., Blockley, S., Staff, R.A., Yamada, K., Kitaba, I., Haraguchi, T., Kitagawa, J. and Smith, V.C., 2020a. Refining the eruptive history of Ulleungdo and Changbaishan volcanoes (East Asia) over the last 86 kyrs using distal sedimentary records. Journal of Volcanology and Geothermal Research, 389: 106669.

McLean, D., Albert, P.G., Suzuki, T., Nakagawa, T., Kimura, J.-I., Chang, Q., Miyabuchi, Y., Manning, C.J., MacLeod, A., Blockley, S.P.E., Staff, R.A., Yamada, K., Kitaba, I., Yamasaki, A., Haraguchi, T., Kitagawa, J., Members, S.P. and Smith, V.C., 2020b.

Constraints on the Timing of Explosive Volcanism at Aso and Aira Calderas (Japan) Between 50 and 30 ka: New Insights From the Lake Suigetsu Sedimentary Record (SG14 Core). Geochemistry, Geophysics, Geosystems, 21(8): e2019GC008874.

Müller, S., Schmidt, M., Kossler, A., Leipe, C., Irino, T., Yamamoto, M., Yonenobu, H., Goslar, T., Kato, H., Wagner, M., Weber, A.W. and Tarasov, P.E., 2016. Palaeobotanical records from Rebun Island and their potential for improving the chronological control and understanding human–environment interactions in the Hokkaido Region, Japan. The Holocene, 26(10): 1646-1660.

Nakamura, Y., 2016. Stratigraphy, distribution, and petrographic properties of Holocene tephras in Hokkaido, northern Japan. Quaternary International, 397: 52-62.

Nakamura, Y. and Hirakawa, K., 2004. Mid-Holocene widespread tephra, Komagatake-g (Ko-g) in Hokkaido, northern Japan. The Quaternary Research (Daiyonki-Kenkyu), 43(3): 189-200 (in Japanese with English abstract).

Okuno, M., Yoshimoto, M., Arai, K.-i., Nakamura, T., Ui, T. and Wada, K., 1999. AMS radiocarbon age of the Ko-f tephra from Hokkaido-Komagatake volcano, southwestern Hokkaido, Japan. Journal of the Geological Society of Japan, 105(5): 364-369 (in Japanese with English abstract).

Oppenheimer, C., Wacker, L., Xu, J., Galván, J.D., Stoffel, M., Guillet, S., Corona, C., Sigl, M., Di Cosmo, N., Hajdas, I., Pan, B., Breuker, R., Schneider, L., Esper, J., Fei, J., Hammond, J.O.S. and Büntgen, U., 2017. Multi-proxy dating the 'Millennium Eruption' of Changbaishan to late 946 CE. Quaternary Science Reviews, 158: 164-171.

Petrie, C.A. and Torrence, R., 2008. Assessing the effects of volcanic disasters on human settlement in the Willaumez Peninsula, Papua New Guinea: a Bayesian approach to radiocarbon calibration. The Holocene, 18(5): 729-744.

Razzhigaeva, N.G., Matsumoto, A. and Nakagawa, M., 2016. Age, source, and distribution of Holocene tephra in the southern Kurile Islands: Evaluation of Holocene eruptive activities in the southern Kurile arc. Quaternary International, 397: 63-78.

Reimer, P.J., Austin, W.E.N., Bard, E., Bayliss, A., Blackwell, P.G., Bronk Ramsey, C., Butzin, M., Cheng, H., Edwards, R.L., Friedrich, M., Grootes, P.M., Guilderson, T.P., Hajdas, I., Heaton, T.J., Hogg, A.G., Hughen, K.A., Kromer, B., Manning, S.W., Muscheler, R., Palmer, J.G., Pearson, C., van der Plicht, J., Reimer, R.W., Richards, D.A., Scott, E.M., Southon, J.R., Turney, C.S.M., Wacker, L., Adolphi, F., Büntgen, U., Capano, M., Fahrni, S.M., Fogtmann-Schulz, A., Friedrich, R., Köhler, P., Kudsk, S., Miyake, F., Olsen, J., Reinig, F., Sakamoto, M., Sookdeo, A. and Talamo, S., 2020. The IntCal20 Northern Hemisphere radiocarbon age calibration curve 0–55 CAL kBP). Radiocarbon: 1-33.

Schiff, C.J., Kaufman, D.S., Wallace, K.L., Werner, A., Ku, T.L. and Brown, T.A., 2008. Modeled tephra ages from lake sediments, base of Redoubt Volcano, Alaska. Quat Geochronol, 3(1-2): 56-67.

Schmidt, M., Tarasov, P.E., Hoelzmann, P., Meyer, H. and Leipe, C., 2016. Diatoms from Lake Kushu: A pilot study to test the potential of a Late Quaternary palaeoenvironmental archive from Rebun Island (Hokkaido Region, Japan). Journal of Asian Earth Sciences, 122: 106-122.

Smith, V.C., Mark, D.F., Staff, R.A., Blockley, S.P.E., Ramsey, C.B., Bryant, C.L., Nakagawa, T., Han, K.K., Weh, A., Takemura, K. and Danhara, T., 2011. Toward establishing precise 40Ar/39Ar chronologies for Late Pleistocene palaeoclimate archives: an example from the Lake Suigetsu (Japan) sedimentary record. Quaternary Science Reviews, 30(21–22): 2845-2850.

Smith, V.C., Staff, R.A., Blockley, S.P.E., Bronk Ramsey, C., Nakagawa, T., Mark, D.F., Takemura, K. and Danhara, T., 2013. Identification and correlation of visible tephras in the Lake Suigetsu SG06 sedimentary archive, Japan: chronostratigraphic markers for synchronising of east Asian/west Pacific palaeoclimatic records across the last 150 ka. Quaternary Science Reviews, 67(0): 121-137.

Sun, C., Németh, K., Zhan, T., You, H., Chu, G. and Liu, J., 2019. Tephra evidence for the most recent eruption of Laoheishan volcano, Wudalianchi volcanic field, northeast China. Journal of Volcanology and Geothermal Research, 383: 103-111.

Sun, C., Wang, L., Plunkett, G., You, H., Zhu, Z., Zhang, L., Zhang, B., Chu, G. and Liu, J., 2018. Ash from the changbaishan qixiangzhan eruption: a new early holocene marker horizon across East Asia. J. Geophys. Res.: Solid Earth, 123: 6442–6450.

Vandergoes, M.J., Hogg, A.G., Lowe, D.J., Newnham, R.M., Denton, G.H., Southon, J., Barrell, D.J.A., Wilson, C.J.N., McGlone, M.S., Allan, A.S.R., Almond, P.C., Petchey, F., Dabell, K., Dieffenbacher-Krall, A.C. and Blaauw, M., 2013. A revised age for the Kawakawa/Oruanui tephra, a key marker for the Last Glacial Maximum in New Zealand. Quaternary Science Reviews, 74: 195–201.

Wohlfarth, B., Blaauw, M., Davies, S.M., Andersson, M., Wastegård, S., Hormes, A. and Possnert, G., 2006. Constraining the age of Lateglacial and early Holocene pollen zones and tephra horizons in southern Sweden with Bayesian probability methods. Journal of Quaternary Science, 21(4): 321-334.

Xu, J., Pan, B., Liu, T., Hajdas, I., Zhao, B., Yu, H., Liu, R. and Zhao, P., 2013. Climatic impact of the Millennium eruption of Changbaishan volcano in China: New insights from high-precision radiocarbon wiggle-match dating. Geophysical Research Letters, 40(1): 54-59.

Yamamoto, T., Ito, J.-i., Nakagawa, M., Hasegawa, T. and Kishimoto, H., 2010. 14 C ages for the ejecta from Kutcharo and Mashu calderas, eastern Hokkaido, Japan. Bulletin of the Geological Survey of Japan, 61(5-6): 161-170 (in Japanese with English abstract).

Yoshimoto, M., Amma-Miyasaka, M., Takahashi, R., Nakagawa, M. and Yoshida, K., 2008. Reevaluation of the pre–1640 AD eruptive history of Hokkaido-Komagatake volcano, northern Japan. Journal of the Geological Society of Japan, 114: 336-347 (in Japanese with English abstract).

Fig. 1 Map of NE Asia showing locations of Komagatake volcano, Mashu caldera, Lake Kushu in Rebun Island and spatial distribution of the Ko-g and Ma-f~j tephras. Solid line indicates that the dispersal limit is based on data from visible tephra studies (Katsui et al., 1975; Machida and Arai, 2003; Furukawa and Nanayama, 2006; Nakamura, 2016; Razzhigaeva et al., 2016), whereas the dashed line is based on data from cryptotephra research (Chen et al., 2019).

Fig. 2 95.4% confidence Highest Probability Density (HPD) output for Bayesian age models for the (a) Ko-g and (b) Ma-f~j tephras. These models utilise the proximal information for the two tephras. The pale distribution for each determination represents the unmodelled ages (*Likelihoods*) derived from the calibration of the radiocarbon dates. The solid distributions show the modelled results after stratigraphic constraints (*Prior*) were implemented within the Bayesian framework. The bars beneath the distributions indicate 95.4% confidence HPD modelled age ranges for each determination. The *Tau_Boundary* function is used to constrain the beginning and the end of the *Sequence* model for the Ko-g tephra, and the beginning of the sequence of the Ma-f~j tephra. The dates between two boundaries are treated as a single group (*Phase*). The dates within each phase are stratigraphically unordered in relation to each other, but the two phases in the Ko-g model have relative stratigraphic order. The values in parentheses after each radiocarbon determination are outlier probabilities [O]. The values of the outlier probability represent both the posterior and prior outlier probabilities given in percent, with the prior outlier probability being defined as 5% for each determination. See the main text for methodological details.

Fig. 3 95.4% confidence Highest Probability Density (HPD) output for Bayesian age model for the Kushu RK12 sequence, with 95.4% confidence HPD modelled age ranges for the Ko-g and Ma-f~j tephras also shown. The model is constructed based on fifty-seven AMS ^{14}C dates from the Kushu RK12 core (Müller et al., 2016), with a high resolution tephra age of the B-Tm tephra (Oppenheimer et al., 2017) inserted in the position where it was identified (Chen et al., 2016). The model utilises a *P_Sequence* deposition model (Bronk Ramsey, 2008), with a variable *k* factor (Bronk Ramsey and Lee, 2013) and outlier analysis (Bronk Ramsey, 2009b), applying the IntCal20 calibration curve (Reimer et al., 2020). The apparent age reversals that were regarded as outliers (see Müller et al., 2016; marked with question marks) are removed from the model. The two *Phase* models of the Ko-g and the Ma-f~j are cross-referenced into the *P_Sequence* based on the identification of these tephras in the record (Chen et al., 2019). In this case, information from both proximal and distal sources together informs the eruption ages. See the main text for methodological details.

Fig. 4 Schematic illustration of age comparison between our final modelled date and the reported eruption ages for the (a) Ko-g and (b) Ma-f~j tephras. The dates in a purple colour indicate that they should no longer be referred to as eruption ages based on our modelling results.

Figure 1

[Click here to access/download;Figure;Fig. 1.pdf]

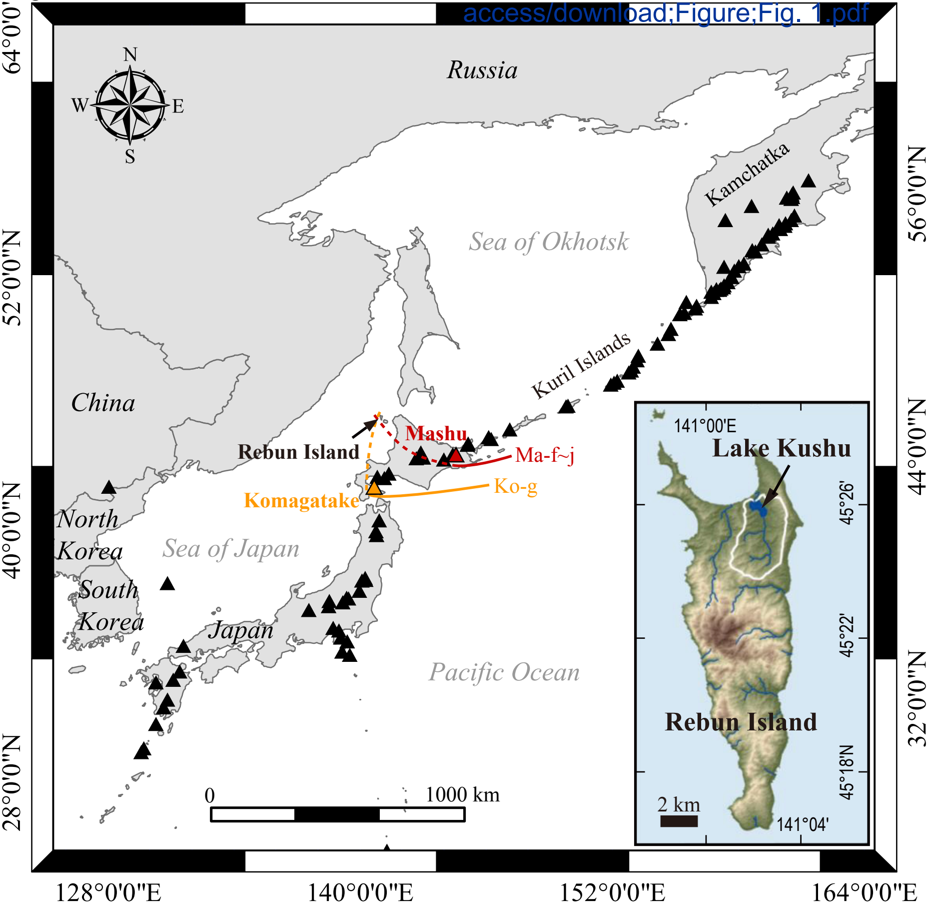

Figure 2

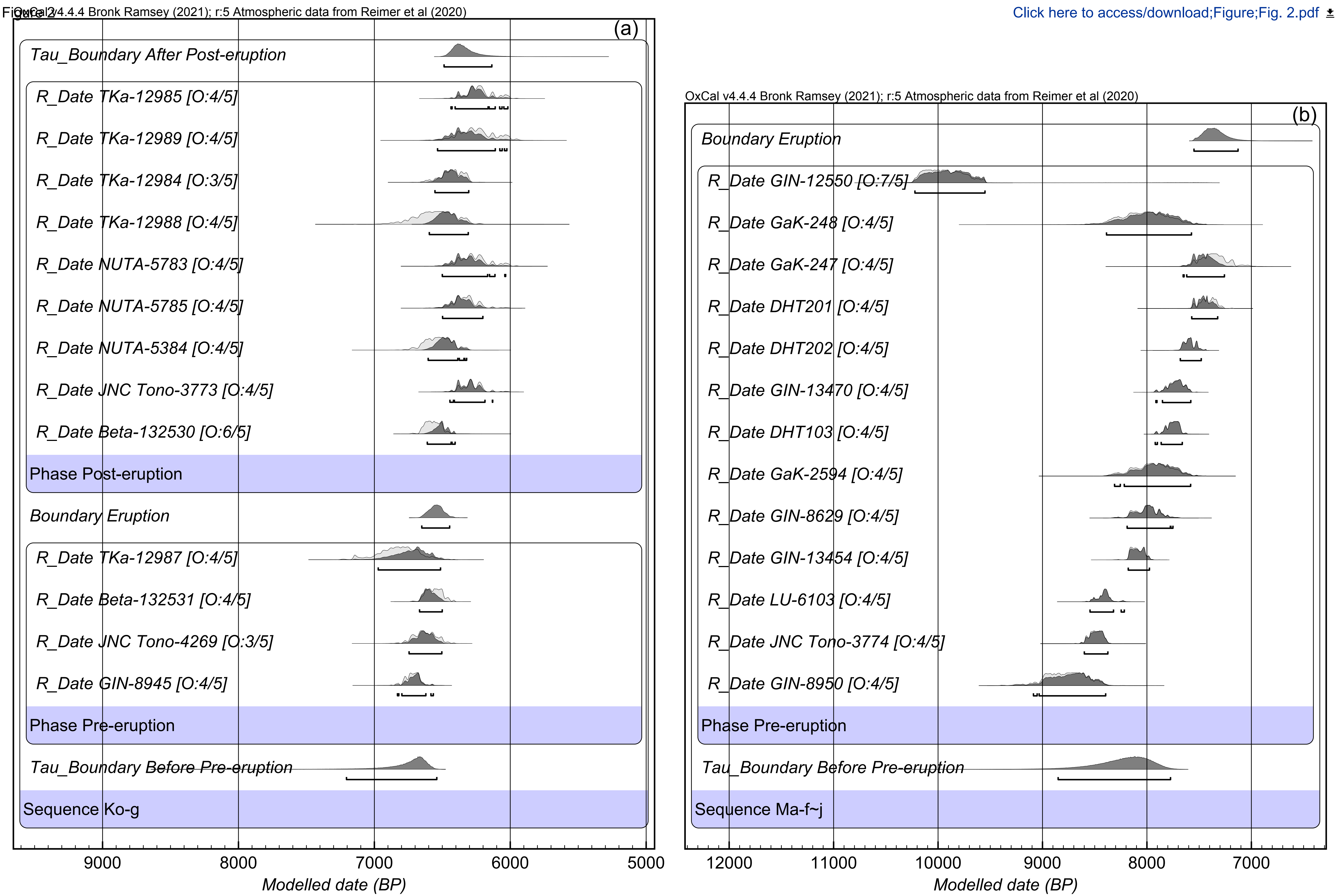
OxCal v4.4.4 Bronk Ramsey (2021); r:5 Atmospheric data from Reimer et al (2020)
(a)
Tau_Boundary After Post-eruption
R_Date TKa-12985 [O:4/5]
R_Date TKa-12989 [O:4/5]
R_Date TKa-12984 [O:3/5]
R_Date TKa-12988 [O:4/5]
R_Date NUTA-5783 [O:4/5]
R_Date NUTA-5785 [O:4/5]
R_Date NUTA-5384 [O:4/5]
R_Date JNC Tono-3773 [O:4/5]
R_Date Beta-132530 [O:6/5]
Phase Post-eruption
Boundary Eruption
R_Date TKa-12987 [O:4/5]
R_Date Beta-132531 [O:4/5]
R_Date JNC Tono-4269 [O:3/5]
R_Date GIN-8945 [O:4/5]
Phase Pre-eruption
Tau_Boundary Before Pre-eruption
Sequence Ko-g
9000
8000
7000
6000
5000
Modelled date (BP)
OxCal v4.4.4 Bronk Ramsey (2021); r:5 Atmospheric data from Reimer et al (2020)
(b)
Boundary Eruption
R_Date GIN-12550 [O:7/5]
R_Date GaK-248 [O:4/5]
R_Date GaK-247 [O:4/5]
R_Date DHT201 [O:4/5]
R_Date DHT202 [O:4/5]
R_Date GIN-13470 [O:4/5]
R_Date DHT103 [O:4/5]
R_Date GaK-2594 [O:4/5]
R_Date GIN-8629 [O:4/5]
R_Date GIN-13454 [O:4/5]
R_Date LU-6103 [O:4/5]
R_Date JNC Tono-3774 [O:4/5]
R_Date GIN-8950 [O:4/5]
Phase Pre-eruption
Tau_Boundary Before Pre-eruption
Sequence Ma-f~j
12000
11000
10000
9000
8000
7000
Modelled date (BP)

Figure 3

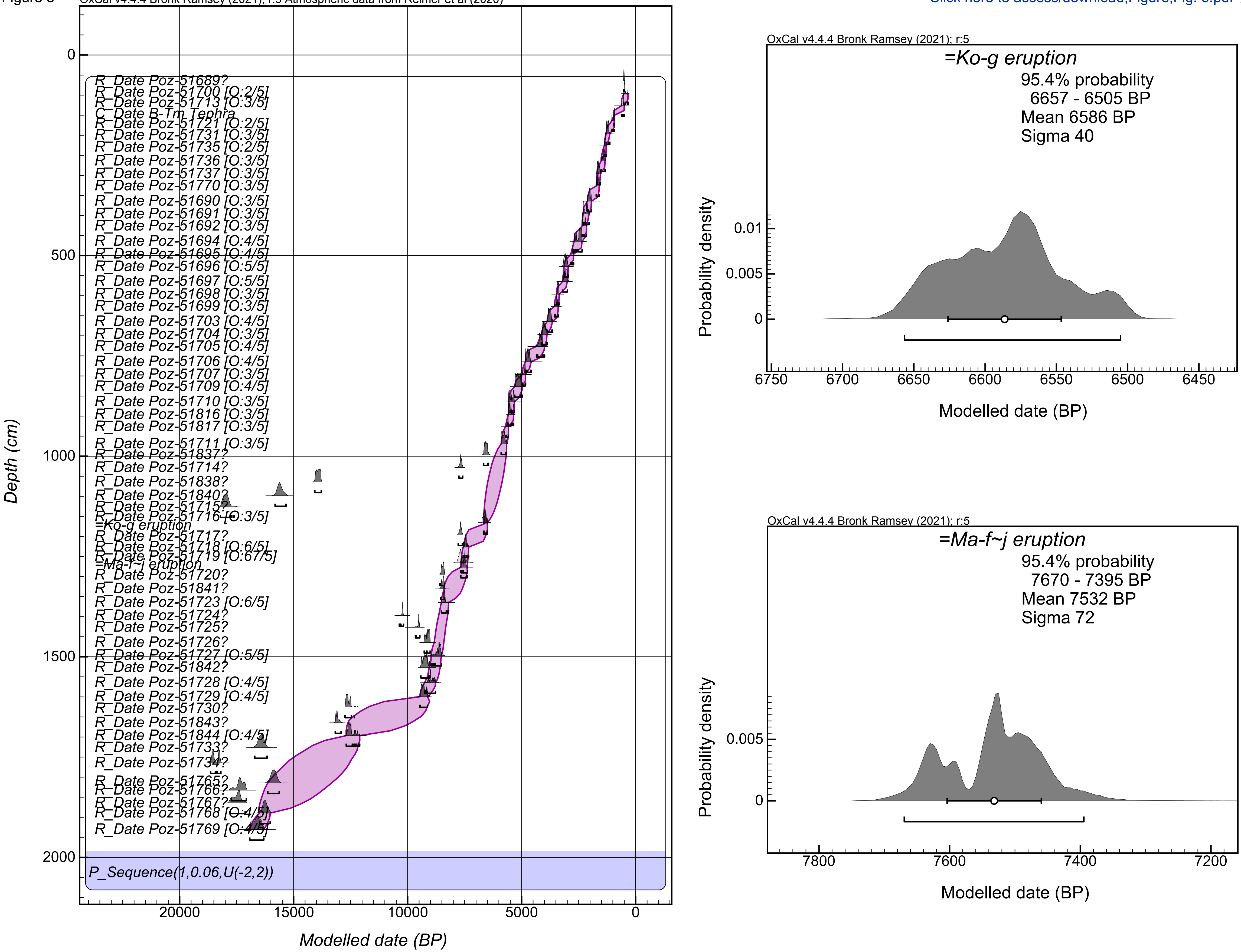

Click here to access/download;Figure;Fig. 3.pdf

Figure 4

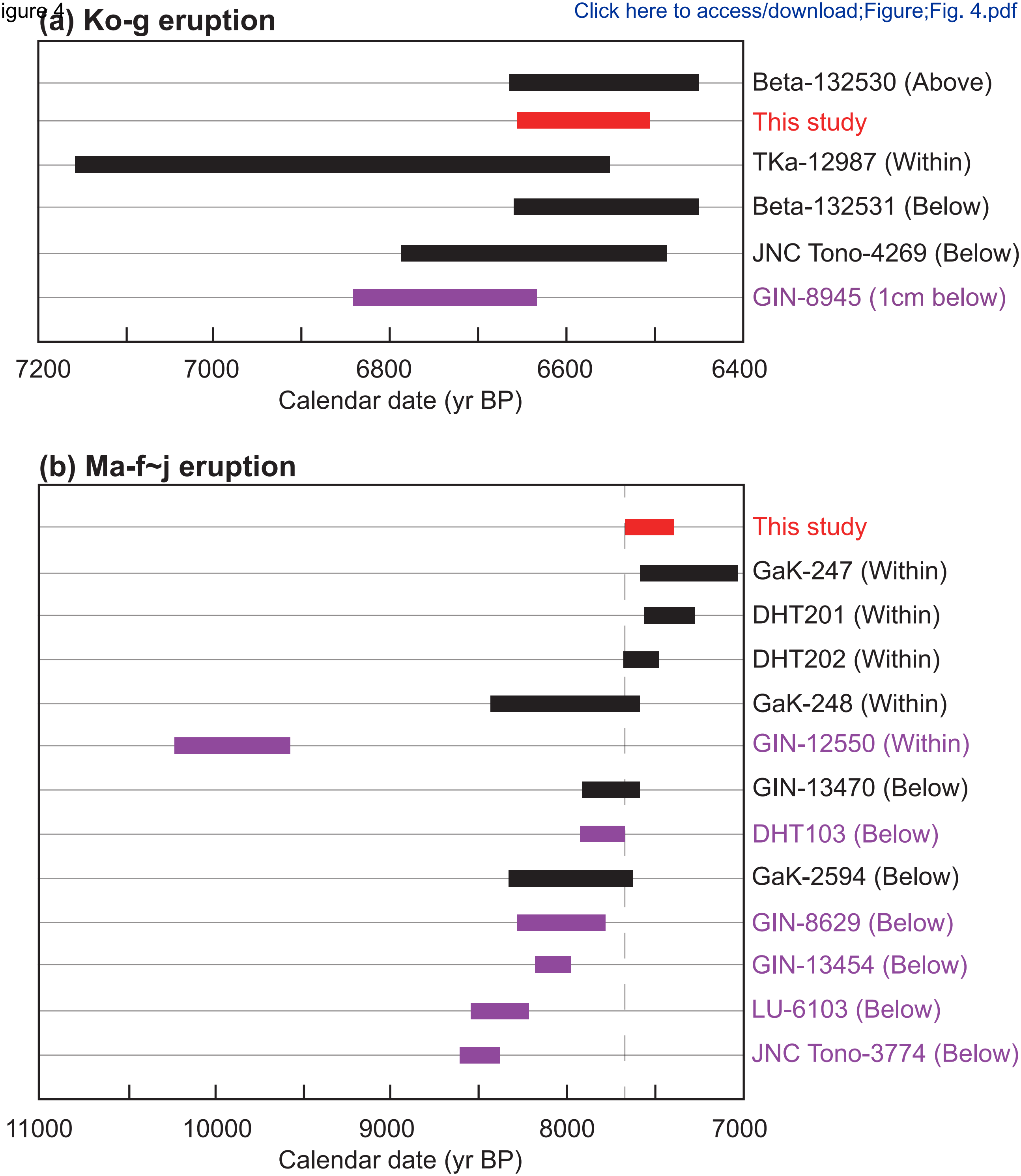
(a) Ko-g eruption
Beta-132530 (Above)
This study
TKa-12987 (Within)
Beta-132531 (Below)
JNC Tono-4269 (Below)
GIN-8945 (1cm below)
7200
7000
6800
6600
6400
Calendar date (yr BP)
(b) Ma-f~j eruption
This study
GaK-247 (Within)
DHT201 (Within)
DHT202 (Within)
GaK-248 (Within)
GIN-12550 (Within)
GIN-13470 (Below)
DHT103 (Below)
GaK-2594 (Below)
GIN-8629 (Below)
GIN-13454 (Below)
LU-6103 (Below)
JNC Tono-3774 (Below)
11000
10000
9000
8000
7000
Calendar date (yr BP)

Conflict of Interest

We confirm that this work is original and has not been published elsewhere nor is it currently under consideration for publication elsewhere. All authors have made substantial contributions to the submission and have approved the final version of the manuscript. We have no conflicts of interest to disclose.

Table 1

Table 1 Summary information of radiocarbon dates used for phase modelling of the Ko-g and Ma-f~j tephras.

Tephra	Material	Stratigraphic relationship with tephra	Lab code	14C date (yr BP)	Uncertainty (1σ)	δ13C (‰)	Re-calibrated date (cal yr BP, 95.4%)	Detailed description	Phase	Reference
Ko-g	Charcoal	Above	TKa-12985	5440	70	-26.0	6394-6003	Charcoal sample within tephra P2 known to be stratigraphically above Ko-g	Post-eruption	Yoshimoto et al., 2008
	Charcoal	Above	TKa-12989	5470	110	-27.6	6489-5995	Charcoal sample within tephra P2 known to be stratigraphically above Ko-g	Post-eruption	Yoshimoto et al., 2008
	Charcoal	Above	TKa-12984	5640	70	-27.3	6621-6295	Charcoal sample within tephra P1 known to be stratigraphically above Ko-g	Post-eruption	Yoshimoto et al., 2008
	Charcoal	Above	TKa-12988	5740	130	-25.0	6849-6291	Charcoal sample within tephra P1 known to be stratigraphically above Ko-g	Post-eruption	Yoshimoto et al., 2008
	Paleosol	Above	NUTA-5783	5480	90	-26.8	6448-6002	Paleosol sample immediately below tephra Ko-f known to be stratigraphically above Ko-g	Post-eruption	Okuno et al., 1999
	Paleosol	Above	NUTA-5785	5530	80	-25.3	6495-6121	Paleosol sample immediately below tephra Ko-f known to be stratigraphically above Ko-g	Post-eruption	Okuno et al., 1999
	Charcoal	Above	NUTA-5384	5730	80	-27.5	6729-6316	Charcoal sample ca. 20 cm above Ko-g	Post-eruption	Okuno et al., 1999
	Humus	Above	JNC Tono-3773	5484	63	-22.98	6435-6029	Humus sample immediately above Ko-g, 13C corrected date	Post-eruption	Nakamura and Hirakawa, 2004
	Plant	Above	Beta-132530	5770	40	-22.6	6667-6452	Plant sample immediately above Ko-g, 13C corrected date	Post-eruption	Nakamura and Hirakawa, 2004
	Charcoal	Within	TKa-12987	5970	110	-28.0	7158-6552	Charcoal sample within bottom part of Ko-g	Pre-eruption	Yoshimoto et al., 2008
	Plant	Below	Beta-132531	5760	40	-22.2	6661-6451	Plant sample immediately below Ko-g, 13C corrected date	Pre-eruption	Nakamura and Hirakawa, 2004
	Wood	Below	JNC Tono-4269	5825	62	-27.34	6787-6486	Wood sample immediately below Ko-g, 13C corrected date	Pre-eruption	Nakamura and Hirakawa, 2004
	N/A	Below	GIN-8945	5900	40	N/A	6844-6635	Unspecified dating material ca. 1 cm below Ko-g	Pre-eruption	Razzhigaeva et al., 2016
Ma-f~j	Charcoal	Within	GaK-247	6460	130	N/A	7590-7024	Charcoal sample within Ma-f unit	Pre-eruption	Katsui, 1963
	Charcoal	Within	DHT201	6510	70	-25.8	7566-7277	Charred material within Ma-f unit	Pre-eruption	Yamamoto et al., 2010
	Charcoal	Within	DHT202	6730	60	-27.7	7681-7483	Charred material within Ma-f unit	Pre-eruption	Yamamoto et al., 2010
	Charcoal	Within	GaK-248	7190	230	N/A	8420-7586	Charcoal sample within Ma-f unit	Pre-eruption	Katsui, 1963
	N/A	Within	GIN-12550	8870	110	N/A	10227-9562	Unspecified dating material within Ma-f~j	Pre-eruption	Razzhigaeva et al., 2016
	N/A	Below	GIN-13470	6880	70	N/A	7916-7584	Unspecified dating material immediately below Ma-f~j	Pre-eruption	Razzhigaeva et al., 2016
	Humus	Below	DHT103	6920	50	-26.1	7920-7666	Charred material from soil immediately below Ma-j unit	Pre-eruption	Yamamoto et al., 2010
	Humic acid	Below	GaK-2594	7120	180	N/A	8326-7619	Humic acid sample immediately below Ma-j unit	Pre-eruption	Katsui et al., 1975
	N/A	Below	GIN-8629	7180	100	N/A	8278-7785	Unspecified dating material immediately below Ma-f~j	Pre-eruption	Razzhigaeva et al., 2016
	N/A	Below	GIN-13454	7270	50	N/A	8180-7978	Unspecified dating material immediately below Ma-f~j	Pre-eruption	Razzhigaeva et al., 2016
	N/A	Below	LU-6103	7610	60	N/A	8545-8221	Unspecified dating material immediately below Ma-f~j	Pre-eruption	Razzhigaeva et al., 2016
	Humus	Below	JNC Tono-3774	7700	69	-22.79	8598-8380	Humus sample immediately below Ma-f unit while Ma-g~j units are missing, 13C corrected date	Pre-eruption	Nakamura and Hirakawa, 2004
	N/A	Below	GIN-8950	7910	140	N/A	9124-8415	Unspecified dating material ca. 10 cm below Ma-f~j	Pre-eruption	Razzhigaeva et al., 2016

Table 2 Summary information of phase and deposition modelling results for the Ko-g and Ma-f~j tephras.

Tephra	RK12 correlative layer	Depth (cm)	Phase modelled date		Deposition modelled date		Final Deposition & phase modelled date	
			95.4%, cal yr BP	μ±σ, cal yr BP	95.4%, cal yr BP	μ±σ, cal yr BP	95.4%, cal yr BP	μ±σ, cal yr BP
Ko-g	RK12-1169	1169	6651-6446	6545±52	7024-6497	6697±137	6657-6505	6586±40
Ma-f~j	RK12-1277	1277	7550-7128	7348±111	8080-7592	7786±128	7670-7395	7532±72